

# Effects of CO<sub>2</sub> Compressibility on CO<sub>2</sub> Storage in Deep Saline Aquifers

Victor Vilarrasa · Diogo Bolster · Marco Dentz ·  
Sebastia Olivella · Jesus Carrera

Received: 3 August 2009 / Accepted: 5 April 2010  
© Springer Science+Business Media B.V. 2010

**Abstract** The injection of supercritical CO<sub>2</sub> in deep saline aquifers leads to the formation of a CO<sub>2</sub> plume that tends to float above the formation brine. As pressure builds up, CO<sub>2</sub> properties, i.e. density and viscosity, can vary significantly. Current analytical solutions do not account for CO<sub>2</sub> compressibility. In this article, we investigate numerically and analytically the effect of this variability on the position of the interface between the CO<sub>2</sub>-rich phase and the formation brine. We introduce a correction to account for CO<sub>2</sub> compressibility (density variations) and viscosity variations in current analytical solutions. We find that the error in the interface position caused by neglecting CO<sub>2</sub> compressibility is relatively small when viscous forces dominate. However, it can become significant when gravity forces dominate, which is likely to occur at late times of injection.

**Keywords** Two phase flow · CO<sub>2</sub> density · Analytical solution · Interface · Gravity forces

## Nomenclature

$c_r$	Rock compressibility
$c_\alpha$	Compressibility of fluid $\alpha$ ( $\alpha = c, w$ )
$d$	Aquifer thickness
$E_{rel}$	Relative error of the interface position
$g$	Gravity
$h_w$	Hydraulic head of water
$k$	Intrinsic permeability
$k_{r\alpha}$	$\alpha$ -Phase relative permeability ( $\alpha = c, w$ )
$N$	Gravity number

---

V. Vilarrasa · M. Dentz · J. Carrera  
Institute of Environmental Assessment and Water Research, GHS, IDAEA, CSIC, Barcelona, Spain

V. Vilarrasa (✉) · D. Bolster · S. Olivella  
Department of Geotechnical Engineering and Geosciences, Technical University of Catalonia (UPC),  
Barcelona, Spain  
e-mail: victor.vilarrasa@upc.edu

$P_{t_0}$	Fluid pressure at the top of the aquifer prior to injection
$P_{DT}$	Fluid pressure for <a href="#">Dentz and Tartakovsky (2009a)</a> approach
$\overline{P}_{DT}$	Vertically averaged fluid pressure for <a href="#">Dentz and Tartakovsky (2009a)</a> approach
$\overline{P}_N$	Vertically averaged fluid pressure for <a href="#">Nordbotten et al. (2005)</a> approach
$\overline{P}_0$	Vertically averaged fluid pressure prior to injection
$P_\alpha$	Fluid pressure of $\alpha$ -phase ( $\alpha = c, w$ )
$Q_m$	CO <sub>2</sub> mass flow rate
$Q_0$	CO <sub>2</sub> volumetric flow rate
$q_\alpha$	Volumetric flux of $\alpha$ -phase ( $\alpha = c, w$ )
$R$	Radius of influence
$R_c$	CO <sub>2</sub> plume radius at the top of the aquifer for compressible CO <sub>2</sub>
$R_i$	CO <sub>2</sub> plume radius at the top of the aquifer for incompressible CO <sub>2</sub>
$r$	Radial distance
$r_0$	CO <sub>2</sub> plume radius at the top of the aquifer
$r_b$	CO <sub>2</sub> plume radius at the base of the aquifer
$r_c$	Characteristic length
$r_w$	Injection well radius
$S_s$	Specific storage coefficient
$S_{rw}$	Residual saturation of the formation brine
$S_\alpha$	Saturation of $\alpha$ -phase ( $\alpha = c, w$ )
$t$	Time
$z$	Vertical coordinate
$z_0$	Depth of the top of the aquifer
$z_b$	Depth of the base of the aquifer
$V$	CO <sub>2</sub> plume volume
$\alpha$	Phase index, c CO <sub>2</sub> and w brine
$\beta$	CO <sub>2</sub> compressibility
$\epsilon_v$	Volumetric strain
$\gamma_{cw}$	A dimensionless parameter that measures the relative importance of viscous and gravity forces
$\lambda_\alpha$	Mobility of $\alpha$ -phase ( $\alpha = c, w$ )
$\mu_\alpha$	Viscosity of $\alpha$ -phase ( $\alpha = c, w$ )
$\rho_0$	CO <sub>2</sub> density at the reference pressure $P_{t_0}$
$\rho_1$	Constant for the CO <sub>2</sub> density
$\overline{\rho}_c$	Mean CO <sub>2</sub> density
$\overline{\rho}_{cDT}$	Mean CO <sub>2</sub> density for <a href="#">Dentz and Tartakovsky (2009a)</a> approach
$\overline{\rho}_{cN}$	Mean CO <sub>2</sub> density for <a href="#">Nordbotten et al. (2005)</a> approach
$\rho_\alpha$	Density of $\alpha$ -phase ( $\alpha = c, w$ )
$\sigma'$	Effective stress
$\phi$	Porosity
$\zeta$	Interface position from the bottom of the aquifer

## 1 Introduction

Carbon dioxide (CO<sub>2</sub>) sequestration in deep geological formations is considered a promising mitigation solution for reducing greenhouse gas emissions to the atmosphere. Although this technology is relatively new, wide experience is available in the field of multiphase fluid injection [e.g. the injection of CO<sub>2</sub> for enhanced oil recovery ([Lake 1989](#);

Cantucci et al. 2009), production and storage of natural gas in aquifers (Dake 1978; Katz and Lee 1990), gravity currents (Huppert and Woods 1995; Lyle et al. 2005) and disposal of liquid waste (Tsang et al. 2008)]. Various types of geological formations can be considered for CO<sub>2</sub> sequestration. These include unminable coal seams, depleted oil and gas reservoirs and deep saline aquifers. The latter have received particular attention due to their high CO<sub>2</sub> storage capacity (Bachu and Adams 2003). Viable saline aquifers are typically at depths greater than 800 m. Pressure and temperature conditions in such aquifers ensure that the density of CO<sub>2</sub> is relatively high (Hitchon et al. 1999).

Several sources of uncertainty associated with multiphase flows exist at these depths. These include those often encountered in other subsurface flows such as the impact of heterogeneity of geological media, e.g. (Neuweiller et al. 2003; Bolster et al. 2009b), variability and lack of knowledge of multiphase flow parameters (e.g. van Genuchten and Brooks–Corey models). Beyond these difficulties, the properties of supercritical CO<sub>2</sub>, such as density and viscosity, can vary substantially (Garcia 2003; Garcia and Pruess 2003; Bachu 2003) making the assumption of incompressibility questionable.

Two analytical solutions have been proposed for the position of the interface between the CO<sub>2</sub>-rich phase and the formation brine: the Nordbotten et al. (2005) solution and the Dentz and Tartakovsky (2009a) solution. Both assume an abrupt interface between phases. Both solutions neglect CO<sub>2</sub> dissolution into the brine, so the effect of convective cells (Ennis-King and Paterson 2005; Hidalgo and Carrera 2009; Riaz et al. 2006) on the front propagation is not taken into account. Each phase has constant density and viscosity. The shape of the solution by Nordbotten et al. (2005) depends on the viscosity of both CO<sub>2</sub> and brine, while the one derived by Dentz and Tartakovsky (2009a) depends on both the density and viscosity differences between the two phases. The validity of these sharp interface solutions has been discussed in, e.g., Dentz and Tartakovsky (2009a); Lu et al. (2009); Dentz and Tartakovsky (2009b).

The injection of CO<sub>2</sub> causes an increase in fluid pressure, and displaces the formation brine laterally. This brine can migrate out of the aquifer if the aquifer is open, causing salinization of other formations such as fresh water aquifers. In contrast, if the aquifer has very low-permeability boundaries, the storage capacity will be related exclusively to rock and fluid compressibility (Zhou et al. 2008). In the latter case, fluid pressure will increase dramatically and this can lead to geomechanical damage of the caprock (Rutqvist et al. 2007). Additionally, this pressure buildup during injection gives rise to a wide range of CO<sub>2</sub> density values within the CO<sub>2</sub> plume (Fig. 1). As density changes are directly related to changes in volume, the interface position will be affected by compressibility. However, neither of the current analytical solutions for the interface location acknowledge changes in CO<sub>2</sub> density.

The evolution of fluid pressure during CO<sub>2</sub> injection has been studied by several authors, e.g. (Saripalli and McGrail 2002; Mathias et al. 2008). Mathias et al. (2008) followed

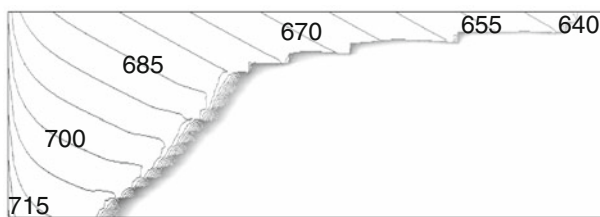


**Fig. 1** CO<sub>2</sub> density (kg/m<sup>3</sup>) within the CO<sub>2</sub> plume resulting from a numerical simulation that acknowledges CO<sub>2</sub> compressibility

Nordbotten et al. (2005), calculating fluid pressure averaged over the thickness of the aquifer. They considered a slight compressibility in the fluids and geological formation, but still assumed constant fluid density values. Accounting for the slight compressibility allows them to avoid the calculation of the radius of influence, which, as we propose later, can be determined by Cooper and Jacob (1946) method.

Typically, CO<sub>2</sub> injection projects are intended to take place over several decades. This implies that the radius of the final CO<sub>2</sub> plume, which can be calculated with the above analytical solutions (Stauffer et al. 2009), may reach the kilometer scale. The omission of compressibility effects can result in a significant error in these estimates. This in turn reduces the reliability of risk assessments, where even simple models can provide a lot of useful information (e.g. Tartakovsky (2007), Bolster et al. (2009a)).

The nature of uncertainty in the density field is illustrated by the Sleipner Project (Korbol and Kaddour 1995). There, around 1 million tones of CO<sub>2</sub> have been injected annually into the Utsira formation since 1996. Nooner et al. (2007) found that the best fit between the gravity measurements made in situ and models based on time-lapse 3D seismic data corresponds to an average in situ CO<sub>2</sub> density of 530 kg/m<sup>3</sup>, with an uncertainty of ± 65 kg/m<sup>3</sup>. This uncertainty is significant in itself. However, prior to these measurements and calculations, the majority of the work on the site had assumed a range between 650–700 kg/m<sup>3</sup>, which implies a significant error (>20%) in volume estimation.

Here, we study the impact of CO<sub>2</sub> compressibility on the interface position, both numerically and analytically. We propose a simple method to account for compressibility effects (density variations) and viscosity variations and apply it to the analytical solutions of Nordbotten et al. (2005) and Dentz and Tartakovsky (2009a). First, we derive an expression for the fluid pressure distribution in the aquifer from the analytical solutions. Then, we propose an iterative method to determine the interface position that accounts for compressibility. Finally, we contrast these corrections with the results of numerical simulations and conclude with a discussion on the importance of considering CO<sub>2</sub> compressibility in the interface position.

## 2 Multiphase Flow: The Role of Compressibility

Consider injection of supercritical CO<sub>2</sub> in a deep confined saline aquifer (see a schematic description in Fig. 2). Momentum conservation is expressed using Darcy’s law, which for phases CO<sub>2</sub>, c, and brine, w, is given by

$$\mathbf{q}_\alpha = -\frac{kk_{r_\alpha}}{\mu_\alpha} (\nabla P_\alpha + \rho_\alpha g \nabla z), \quad \alpha = c, w, \tag{1}$$

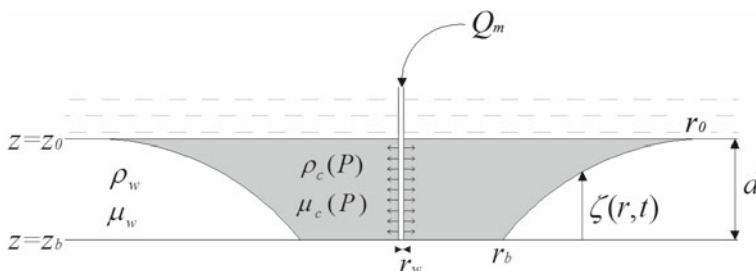


Fig. 2 Problem setup. Injection of compressible CO<sub>2</sub> in a homogeneous horizontal deep saline aquifer

where  $\mathbf{q}_\alpha$  is the volumetric flux of  $\alpha$ -phase,  $k$  is the intrinsic permeability,  $k_{r_\alpha}$  is the  $\alpha$ -phase relative permeability,  $\mu_\alpha$  its viscosity,  $P_\alpha$  its pressure,  $\rho_\alpha$  its density,  $g$  is gravity and  $z$  is the vertical coordinate.

Mass conservation of these two immiscible fluids can be expressed as (Bear 1972),

$$\frac{\partial(\rho_\alpha S_\alpha \phi)}{\partial t} = -\nabla \cdot (\rho_\alpha \mathbf{q}_\alpha), \tag{2}$$

where  $S_\alpha$  is the saturation of the  $\alpha$ -phase,  $\phi$  is the porosity of the porous medium and  $t$  is time.

The left-hand side of Eq. (2) represents the time variation of the mass of  $\alpha$ -phase per unit volume of porous medium. Assuming that there is no external loading, and that the grains of the porous medium are incompressible, but not stationary (Bear 1972), the expansion of the partial derivative of this term results in

$$\frac{\partial(\rho_\alpha S_\alpha \phi)}{\partial t} = S_\alpha \phi \rho_\alpha c_\alpha \frac{\partial P_\alpha}{\partial t} + \rho_\alpha S_\alpha c_r \frac{\partial P_\alpha}{\partial t} + \rho_\alpha \phi \frac{\partial S_\alpha}{\partial t}. \tag{3}$$

where  $c_\alpha = (1/\rho_\alpha)(d\rho_\alpha/dP_\alpha)$  is fluid compressibility,  $c_r = d\epsilon_v/d\sigma'$  is rock compressibility,  $\epsilon_v$  is the volumetric strain and  $\sigma'$  is the effective stress.

The first term in the right-hand side of Eq. (3) corresponds to changes in storage caused by the compressibility of fluid phases. The second term refers to rock compressibility. The third term in the right-hand side of Eq. (3) represents changes in the mass of  $\alpha$  caused by fluid saturation–desaturation processes (i.e. CO<sub>2</sub> plume advance). As such, it does not represent compressibility effects, although its actual value will be sensitive to pressure through the phase density, which controls the size of the CO<sub>2</sub> plume.

The relative importance of the first two terms depends on whether we are in the CO<sub>2</sub> or brine zones, because the compressibility of CO<sub>2</sub> is much larger than that of brine and rock. Typical rock compressibility values at depths of interest for CO<sub>2</sub> sequestration range from  $10^{-11}$  to  $5 \times 10^{-9} \text{ Pa}^{-1}$  (Neuzil 1986), but can be effectively larger if plastic deformation conditions are reached. Water compressibility is of the order of  $4.5 \times 10^{-10} \text{ Pa}^{-1}$ , which lies within the range of rock compressibility values. CO<sub>2</sub> compressibility ranges from  $10^{-9}$  to  $10^{-8} \text{ Pa}^{-1}$  (Law and Bachu 1996; Span and Wagner 1996), one to two orders of magnitude greater than that of rock and water. Thus, CO<sub>2</sub> compressibility has a significant effect on the first term in the right-hand side of Eq. (3). However, the second term, which accounts for rock compressibility, can be neglected in the CO<sub>2</sub>-rich zone, both because it is small and because the volume of rock occupied by CO<sub>2</sub> is orders of magnitude smaller than that affected by pressure buildup of the formation brine.

The situation is different in the region occupied by resident water. Water compressibility is at the low end of rock compressibilities at large depths. Moreover, its value is multiplied by porosity. Therefore, water compressibility will only play a relevant role in high porosity stiff rocks, which are rare. In any case, the two compressibility terms can be combined in the brine saturated zone, yielding

$$\rho_w g (\phi c_w + c_r) \frac{\partial h_w}{\partial t} = S_s \frac{\partial h_w}{\partial t}, \tag{4}$$

where  $h_w$  is the hydraulic head of water, and  $S_s$  is the specific storage coefficient (Bear 1972), which accounts for both brine and rock compressibility.

The specific storage coefficient controls, together with permeability, the radius of influence,  $R$  (i.e. the size of the pressure buildup cone caused by injection). In fact, assuming the aquifer to be large and for the purpose of calculating pressure buildup, this infinite compressible system can be replaced by an incompressible system whose radius grows as determined

from the comparison between Thiem's solution (steady state) (Thiem 1906) and Jacob's solution (transient) (Cooper and Jacob 1946)

$$\Delta P_w = \frac{Q_0 \mu_w}{4\pi k d} \ln \left( \frac{R^2}{r^2} \right) = \frac{Q_0 \mu_w}{4\pi k d} \ln \left( \frac{2.25 k \rho_w g t}{\mu_w r^2 S_s} \right), \quad (5)$$

where  $Q_0$  is the volumetric flow rate,  $\mu_w$  is the viscosity of water,  $k$  is the intrinsic permeability of the aquifer,  $d$  is the aquifer thickness and  $r$  is radial distance. The radius of influence can then be defined from Eq. (5) as

$$R = \sqrt{\frac{2.25 k \rho_w g t}{\mu_w S_s}}. \quad (6)$$

CO<sub>2</sub> is lighter than brine and density differences affect flow via buoyancy. To quantify the relative influence of buoyancy we define a gravity number,  $N$ , as the ratio of gravity to viscous forces. The latter can be represented by the horizontal pressure gradient ( $Q_0 \mu / (2\pi k r d)$ ), and the former by the buoyancy force ( $\Delta \rho g$ ) in Darcy's law, expressed in terms of equivalent head. This would yield the traditional gravity number for incompressible flow (e.g. Lake 1989). However, for compressible fluids, the boundary condition is usually expressed in terms of the mass flow rate,  $Q_m$  (Fig. 2). Therefore, it is more appropriate to write  $Q_0$  as  $Q_m / \rho$ . Hence,  $N$  becomes

$$N = \frac{k \Delta \rho g \bar{\rho}_c 2\pi r_c d}{\mu_c Q_m}, \quad (7)$$

where  $\Delta \rho$  is the difference between the fluids density,  $\bar{\rho}_c$  is a characteristic density,  $r_c$  is a characteristic length and  $Q_m$  is the CO<sub>2</sub> mass flow rate. Large gravity numbers ( $N \gg 1$ ) indicate that gravity forces dominate. Small gravity numbers ( $N \ll 1$ ) indicate that viscous forces dominate. Gravity numbers close to one indicate that gravity and viscous forces are comparable.

The characteristic density can be chosen as the mean CO<sub>2</sub> density of the plume. The characteristic length depends on the scale of interest (Kopp et al. 2009). The gravity number increases with the characteristic length, thus increasing the relative importance of gravity forces with respect to viscous forces (Tchelepi and Orr Jr. 1994). This implies that, as the CO<sub>2</sub> plume becomes large, gravity forces will dominate far from the injection well.

These equations can be solved numerically, e.g. (Aziz and Settari 2002; Chen et al. 2006; Pruess et al. 2004). However, creating a numerical model for each potential candidate site may require a significant cost. Alternatively, the problem can be solved analytically using some simplifications. The use of analytical solutions is useful because (i) they are instantaneous (Stauffer et al. 2009), (ii) numerical solutions can be coupled with analytical solutions to make them more efficient (Celia and Nordbotten 2009) and (iii) they identify important scaling relationships that give insight into the balance of the physical driving mechanisms.

### 3 Analytical Solutions

#### 3.1 Abrupt Interface Approximation

The abrupt interface approximation considers that the two fluids, CO<sub>2</sub> and brine in this case, are immiscible and separated by a sharp interface. The saturation of each fluid is assumed

constant in each fluid region and capillary effects are usually neglected. Neglecting compressibility and considering a quasi-steady (successive steady-states) description of moving fronts in Eq. (2) yields that the volumetric flux defined in (1) is divergence free. In addition, if the Dupuit assumption is adopted in a horizontal radial aquifer and  $S_\alpha$  is set to 1, i.e. the  $\alpha$ -phase relative permeability equals 1, the following equation can be derived (Bear 1972)

$$\frac{1}{r} \frac{\partial}{\partial r} \left[ \zeta \frac{Q_0 - 2\pi r \Delta \rho g (k/\mu_c) (d - \zeta) \partial \zeta / \partial r}{\zeta + (d - \zeta) \mu_w / \mu_c} \right] + 2\pi \phi \frac{\partial \zeta}{\partial t} = 0, \tag{8}$$

where  $\zeta$  is the distance from the base of the aquifer to the interface position and  $Q_0$  is the volumetric flow rate. To account for a residual saturation of the formation brine,  $S_{r_w}$ , behind the CO<sub>2</sub> front, one should replace  $\mu_c$  by  $\mu_c / k'_{rc}$  in Eq. (8) and below, where  $k'_{rc}$  is the CO<sub>2</sub> relative permeability evaluated at the residual brine saturation  $S_{r_w}$ . Equation (8) can be expressed in dimensionless form using

$$r_D = \frac{r}{r_c}, \quad \zeta_D = \frac{\zeta}{d}, \quad t_D = \frac{t}{t_c}, \quad M = \frac{k_{r_w} / \mu_w}{k_{r_c} / \mu_c}, \quad N, \tag{9}$$

where  $M$  is the mobility ratio,  $N$  is the gravity number defined in Eq. (7),  $t_c$  is the characteristic time and the subscript D denotes a dimensionless variable, which yields

$$\frac{1}{r_D} \frac{\partial}{\partial r_D} \left[ \zeta_D \frac{1 - r_D N (d/r_c) (1 - \zeta_D) \partial \zeta_D / \partial r_D}{\zeta_D + (1 - \zeta_D) / M} \right] + \frac{\partial \zeta_D}{\partial t_D} = 0. \tag{10}$$

Equation (10) shows that the problem depends on two parameters,  $N$  and  $M$ . The mobility ratio will have values around 0.1 for CO<sub>2</sub> sequestration, which will lead to the formation of a thin layer of CO<sub>2</sub> along the top of the aquifer (Hesse et al. 2007, 2008; Juanes et al. 2009). On the other hand, the gravity number can vary over several orders of magnitude, depending on the aquifer permeability and the injection rate. Thus, the gravity number is the key parameter governing the interface position.

The analytical solutions of Nordbotten et al. (2005) and Dentz and Tartakovsky (2009a) to determine the interface position of the CO<sub>2</sub> plume when injecting supercritical CO<sub>2</sub> in a deep saline aquifer start from this approximation.

### 3.2 Nordbotten et al. (2005) Approach

To find the interface position, Nordbotten et al. (2005) solve Eq. (8) neglecting the gravity term and approximating the transient system response to injection into an infinite aquifer by a solution to the steady-state problem with a moving outer boundary whose location increases in proportion to  $\sqrt{t}$  in a radial geometry, i.e. the radius of influence defined in (6). In addition, they impose (i) volume balance, (ii) gravity override (CO<sub>2</sub> plume travels preferentially along the top) and (iii) they minimize energy at the well. The fluid pressure applies over the entire thickness of the aquifer and fluid properties are vertically averaged. The vertically averaged properties are defined as a linear weighting between the properties of the two phases. Nordbotten et al. (2005) write their solution as a function of the mobility,  $\lambda_\alpha$ , defined as the ratio of relative permeability to viscosity,  $\lambda_\alpha = k_{r_\alpha} / \mu_\alpha$ . For the case of an abrupt interface where both sides of the interface are fully saturated with the corresponding phase, the relative permeability is 1 and  $\lambda$  becomes the inverse of the viscosity of each phase. These viscosities are assumed constant.

Under these assumptions, Nordbotten et al. (2005) obtain the interface position as,

$$\zeta_N(r, t) = d \left[ 1 - \frac{\mu_c}{\mu_w - \mu_c} \left( \sqrt{\frac{\mu_w V(t)}{\mu_c \phi \pi d r^2}} - 1 \right) \right], \quad (11)$$

where  $V(t) = Q_0 \cdot t$  is the CO<sub>2</sub> volume assuming a constant CO<sub>2</sub> density.

Integrating the flow equation and assuming vertically integrated properties of the fluid over the entire thickness of the formation, Nordbotten et al. (2005) provide the following expression for fluid pressure buildup

$$\bar{P}_N(r, t) - \bar{P}_0 = \frac{Q_0 \mu_w}{2\pi k} \int_r^R \frac{dr}{r \left[ \left( \frac{\mu_w - \mu_c}{\mu_c} \right) (d - \zeta(r)) + d \right]}, \quad (12)$$

where  $\bar{P}_N$  is the vertically averaged pressure,  $\bar{P}_0$  is the vertically averaged initial pressure prior to injection,  $Q_0$  is the volumetric CO<sub>2</sub> injection flow rate,  $k$  is the intrinsic permeability of the aquifer,  $r$  is the radial distance and  $R$  is the radius of influence.

### 3.3 Dentz and Tartakovsky (2009a) Approach

Dentz and Tartakovsky (2009a) also consider an abrupt interface approximation. They include buoyancy effects, and the densities and viscosities of each phase are assumed constant.

They combine Darcy's law with the Dupuit assumption in radial coordinates. Imposing fluid pressure continuity at the interface they obtain

$$\zeta_{DT}(r, t) = d \gamma_{cw} \ln \left[ \frac{r}{r_b(t)} \right], \quad (13)$$

where  $r_b$  is the radius of the interface at the base of the aquifer, and  $\gamma_{cw}$  is a dimensionless parameter that measures the relative importance of viscous and gravity forces

$$\gamma_{cw} = \frac{Q_0}{2\pi k d^2 g} \frac{\Delta\mu}{\Delta\rho}, \quad (14)$$

where  $\Delta\mu = \mu_w - \mu_c$  is the difference between fluid viscosities and  $\Delta\rho = \rho_w - \rho_c$  is the difference between fluid densities.

The interface radius at the base of the aquifer is obtained from volume balance as

$$r_b(t) = \sqrt{\frac{2Q_0 t}{\pi \phi d \gamma_{cw}} \left[ \exp \left( \frac{2}{\gamma_{cw}} \right) - 1 \right]^{-1}}. \quad (15)$$

Note that the fluid viscosity contrast is treated differently in the two approaches (i.e. mobility ratio and viscosity difference). The mobility ratio is particularly relevant in multiphase flow when the two phases coexist. However, when one phase displaces the other, the viscosity difference governs the process (see Eq. (14) in Dentz and Tartakovsky (2009a) solution). An exception to this is the case when fluid properties are integrated vertically (Nordbotten et al. 2005), which can be thought of as a coexistence of phases.



### 4 Compressibility Correction

Let us assume that we have an initial estimation of the mean CO<sub>2</sub> density and viscosity. With this we can calculate the interface position using either analytical solutions (11) or (13). Furthermore, the fluid pressure can be calculated from Darcy’s law. Then, the density can be determined within the plume assuming that it is solely a function of pressure. Integrating the CO<sub>2</sub> density within the plume and dividing it by the volume of the plume, we obtain the mean CO<sub>2</sub> density

$$\bar{\rho}_c = \frac{1}{V} \int_0^d \int_0^{r(\zeta)} 2\pi \phi r \rho_c(P_c) dr dz, \tag{16}$$

where  $V$  is the volume occupied by the CO<sub>2</sub> plume and  $r(\zeta)$  is the distance from the well to the interface position from either Nordbotten et al. (2005) or Dentz and Tartakovsky (2009a).

Note here that we do not specify a priori a particular relationship between density and pressure. We only specify that density is solely a function of pressure. CO<sub>2</sub> density also depends on temperature (Garcia 2003). However, we neglect thermal effects within the aquifer, and take the mean temperature of the aquifer as representative of the system. This assumption is commonly used in CO<sub>2</sub> injection simulations (e.g. Law and Bachu (1996); Pruess and Garcia (2002)) and may be considered valid if CO<sub>2</sub> does not expand rapidly. If this happens, CO<sub>2</sub> will experience strong cooling due to the Joule–Thomson effect.

The relationship between pressure and density in Eq. (16) is in general non-linear. Moreover, pressure varies in space. Notice that the dependence is two-way: CO<sub>2</sub> density depends explicitly on fluid pressure, but fluid pressure also depends on density, because density controls the plume volume, and thus the fluid pressure through the volume of water that needs to be displaced. Therefore, an iterative scheme is needed to solve this non-linear problem. As density varies moderately with pressure, a Picard algorithm should converge, provided that the initial approximation is not too far from the solution.

The formulation of this iterative approach requires an expression for the spatial variability of fluid pressure for each of the two analytical solutions. In the approach of Nordbotten et al. (2005), we obtain an expression for the vertically averaged pressure by introducing (11) into (12) and integrating. The expression for pressure depends on the region: close to the injection well, all fluid is CO<sub>2</sub>; far away, all fluid is saline water; in between the two phases coexist with an abrupt interface between them,

$$\begin{aligned} r > r_0; \quad \bar{P}_N(r, t) &= \bar{P}_0 + \frac{Q_0 \mu_w}{2\pi kd} \ln\left(\frac{R}{r}\right), \\ r_b \leq r \leq r_0; \quad \bar{P}_N(r, t) &= \bar{P}_0 + \frac{Q_0 \mu_w}{2\pi kd} \left[ \ln\left(\frac{R}{r_0}\right) + \sqrt{\frac{\mu_c \phi \pi d}{\mu_w V(t)}} (r_0 - r) \right], \\ r < r_b; \quad \bar{P}_N(r, t) &= \bar{P}_0 + \frac{Q_0 \mu_w}{2\pi kd} \left[ \ln\left(\frac{R}{r_0}\right) + \sqrt{\frac{\mu_c \phi \pi d}{\mu_w V(t)}} (r_0 - r_b) + \frac{\mu_c}{\mu_w} \ln\left(\frac{r_b}{r}\right) \right], \end{aligned} \tag{17}$$

where  $r_0$  is the radial distance where the interface intersects the top of the aquifer,  $r_b$  is the radial distance where the interface intersects the bottom of the aquifer,  $\bar{P}_0 = P_{t_0} + \rho_w g d/2$  is the vertically averaged fluid pressure prior to injection, and  $P_{t_0}$  is the initial pressure at the top of the aquifer. Mathias et al. (2008) come to a similar expression for fluid pressure, but

they consider a slight compressibility in the fluids and rock instead of a radius of influence. The vertically averaged fluid pressure varies with the logarithm of the distance to the well in the regions where a single phase is present (CO<sub>2</sub> or brine). However, it varies linearly in the region where both phases coexist.

Fluid pressure can be obtained from the [Dentz and Tartakovsky \(2009a\)](#) approach by integrating (1), assuming hydrostatic pressure (Dupuit approximation) in the aquifer, and taking the interface position given by (13), which yields

$$\begin{aligned}
 r > r(\zeta_{\text{DT}}); \quad P_{\text{DT}}(r, z, t) &= P_{t_0} + \rho_w g(d - z) + \frac{Q_0 \mu_w}{2\pi k d} \ln\left(\frac{R}{r}\right), \\
 r \leq r(\zeta_{\text{DT}}); \quad P_{\text{DT}}(r, z, t) &= P_{t_0} + \rho_w g(d - z) + \frac{Q_0}{2\pi k d} \\
 &\quad \times \left( \mu_w \ln\left(\frac{R}{r_b}\right) + \mu_c \ln\left(\frac{r_b}{r}\right) - (\mu_w - \mu_c) \frac{z}{d\gamma_{\text{cw}}} \right). \quad (18)
 \end{aligned}$$

Equation (18) can be averaged over the entire thickness of the aquifer to obtain an averaged pressure, which will be used to compare the two approaches. This averaged pressure is given by

$$\begin{aligned}
 r > r_0; \quad \bar{P}_{\text{DT}}(r, t) &= \bar{P}_0 + \frac{Q_0 \mu_w}{2\pi k d} \ln\left(\frac{R}{r}\right), \\
 r_b \leq r \leq r_0; \quad \bar{P}_{\text{DT}}(r, t) &= \bar{P}_0 + \frac{Q_0}{2\pi k d} \left[ \mu_w \left[ \ln\left(\frac{R}{r_b}\right) + \gamma_{\text{cw}} \ln\left(\frac{r}{r_b}\right) \ln\left(\frac{r_b}{r}\right) \right] \right. \\
 &\quad \left. + \mu_c \ln\left(\frac{r_b}{r}\right) \left[ 1 - \gamma_{\text{cw}} \ln\left(\frac{r}{r_b}\right) \right] \right. \\
 &\quad \left. - \frac{\mu_w - \mu_c}{2\gamma_{\text{cw}}} \left[ 1 - \gamma_{\text{cw}}^2 \left( \ln\left(\frac{r}{r_b}\right) \right)^2 \right] \right], \\
 r < r_b; \quad \bar{P}_{\text{DT}}(r, t) &= \bar{P}_0 + \frac{Q_0}{2\pi k d} \left[ \mu_w \ln\left(\frac{R}{r_b}\right) + \mu_c \ln\left(\frac{r_b}{r}\right) - \frac{\mu_w - \mu_c}{2\gamma_{\text{cw}}} \right]. \quad (19)
 \end{aligned}$$

Thus, the vertically averaged fluid pressure is defined in three regions in both approaches by Eqs. (17) and (19). Unsurprisingly, the two approaches have the same solution in the regions where only one phase exists. Differences appear in the region where CO<sub>2</sub> and the formation brine coexist. In the [Nordbotten et al. \(2005\)](#) approach, the vertically averaged pressure varies linearly with distance to the well. However, in [Dentz and Tartakovsky \(2009a\)](#), it changes logarithmically with distance to the well. As a result, the approach of [Dentz and Tartakovsky \(2009a\)](#) predicts higher fluid pressure values in this zone.

Equations (17) and (18) allow us to develop a simple iterative method for correcting the interface position. The method can be applied to both the [Nordbotten et al. \(2005\)](#) and [Dentz and Tartakovsky \(2009a\)](#) solutions as well as to any other future solutions that may emerge. The procedure is as follows

1. Take a reasonable initial approximation for mean CO<sub>2</sub> density and viscosity from the literature, e.g. [Bachu \(2003\)](#).
2. Determine the interface position using mean density and viscosity in analytical solutions (11) or (13).
3. Calculate the pressure distribution using (17) or (18).
4. Calculate the corresponding mean density and viscosity of the CO<sub>2</sub> using (16).

5. Repeat steps 2–4 until the solution converges to within some prespecified tolerance. Two different convergence criteria can be chosen: (i) changes in the interface position, or (ii) changes in the mean CO<sub>2</sub> density.

The method is relatively easy to implement and can be programmed in a spreadsheet or any code of choice. The method converges rapidly, within a few iterations (typically less than 5) in all test cases. A calculation spreadsheet can be downloaded from [GHS \(2009\)](#).

## 5 Application

### 5.1 Injection Scenarios

To illustrate the relevance of CO<sub>2</sub> compressibility effects, we consider three injection scenarios: (i) a regime in which viscous forces dominate gravity forces, (ii) one where both forces have a similar influence and (iii) a case where gravity forces dominate.

CO<sub>2</sub> thermodynamic properties have been widely investigated, e.g. ([Sovova and Prochazka 1993](#); [Span and Wagner 1996](#); [Garcia 2003](#)). The thermodynamic properties given by [Span and Wagner \(1996\)](#) are almost identical to the International Union of Pure and Applied Chemistry (IUPAC) ([Angus et al. 1976](#)) data sets over the  $P - T$  range of CO<sub>2</sub> sequestration interest ([McPherson et al. 2008](#)). However, the algorithm given by [Span and Wagner \(1996\)](#) for evaluating CO<sub>2</sub> properties has a very high computational cost. For the sake of simplicity and illustrative purposes, we assume a linear relationship between CO<sub>2</sub> density and pressure, given as

$$\rho_c = \rho_0 + \rho_1 \beta (P_c - P_{t_0}), \quad (20)$$

where  $\rho_0$  and  $\rho_1$  are constants for the CO<sub>2</sub> density,  $\beta$  is the CO<sub>2</sub> compressibility,  $P_c$  is CO<sub>2</sub> pressure and  $P_{t_0}$  is the reference pressure for  $\rho_0$ .  $\rho_0$ ,  $\rho_1$  and  $\beta$  are obtained from data tables in [Span and Wagner \(1996\)](#). Appendix A contains the expressions for the mean CO<sub>2</sub> density using this linear approximation in (20) for both approaches.

CO<sub>2</sub> viscosity is calculated using an expression proposed by [Altunin and Sakhabetdinov \(1972\)](#). In this expression, the viscosity is a function of density and temperature. Thus the mean CO<sub>2</sub> viscosity is calculated from the mean CO<sub>2</sub> density. Figure 3 shows how the density varies within the CO<sub>2</sub> plume for one of our numerical simulations. The numerical simulations calculate CO<sub>2</sub> density by means of an exponential function ([Span and Wagner 1996](#))

**Fig. 3** CO<sub>2</sub> pressure and CO<sub>2</sub> density at the top of the aquifer resulting from a numerical simulation that acknowledges CO<sub>2</sub> compressibility

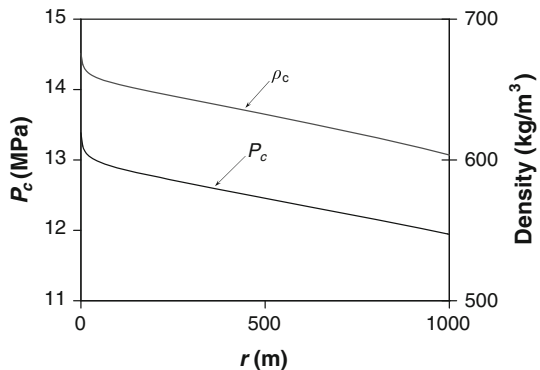


**Table 1** Parameters considered for the numerical simulations in the three injection scenarios

	$\lambda$	$P_o$ (Mpa)	$k$ (m <sup>2</sup> )	$k_{r\alpha}$	$Q_m$ (kg/s)	$r_w$ (m)	$S$
Case 1			$10^{-13}$		120		
Case 2	0.8	0.02	$10^{-12}$	$S_\alpha$	79	0.15	0.0001
Case 3			$10^{-12}$		1		

and CO<sub>2</sub> viscosity using the same expression as here (Altunin and Sakhabetdinov 1972). The maximum error encountered in this study due to the linear CO<sub>2</sub> density approximation was around 8%, which we deem acceptable for our illustrative purposes. Bachu (2003) shows vertical profiles of CO<sub>2</sub> density assuming hydrostatic pressure and different geothermal gradients. However, pressure buildup affects CO<sub>2</sub> properties. Hence, these vertical profiles can only be taken as a reference, for example, to obtain the initial approximation of CO<sub>2</sub> density and viscosity.

We study a saline aquifer at a depth that ranges from 1000 to 1100 m. The temperature is assumed to be constant and equal to 320 K. For this depth and temperature, the initial CO<sub>2</sub> density is estimated as 730 kg/m<sup>3</sup> (Bachu 2003). The corresponding CO<sub>2</sub> viscosity according to Altunin and Sakhabetdinov is 0.061 mPa·s.

For the numerical simulations we used the program CODE\_BRIGHT (Olivella et al. 1994, 1996) with the incorporation of the above defined constitutive equations for CO<sub>2</sub> density and viscosity. This code solves the mass balance of water and CO<sub>2</sub> (Eq. (2)) using the finite element method and a Newton–Raphson scheme to solve the nonlinearities. The aquifer is represented by an axisymmetric model in which a constant CO<sub>2</sub> mass rate is injected uniformly in the whole vertical of the well. The aquifer is assumed infinite-acting, homogeneous and isotropic. In order to obtain a solution close to an abrupt interface, a van Genuchten retention curve (van Genuchten 1980), with an entry pressure,  $P_o$ , of 0.02 MPa and the shape parameter  $\lambda = 0.8$ , was used. To approximate a sharp interface, linear relative permeability functions, for both the CO<sub>2</sub> and the brine, have been used (Table 1). This retention curve and relative permeability functions enable us to obtain a CO<sub>2</sub>-rich zone with a saturation very close to 1, and a relatively narrow mixing zone. The CO<sub>2</sub> saturation 90% iso-line has been chosen to represent the position of the interface.

## 5.2 Case 1: Viscous Forces Dominate

This first case consists of an injection with a gravity number of the order of  $10^{-3}$  in the well. In this situation, the corrected mean CO<sub>2</sub> density (770 kg/m<sup>3</sup> for Nordbotten et al. (2005) and 803 kg/m<sup>3</sup> for Dentz and Tartakovsky (2009a)) is higher than that assumed initially (730 kg/m<sup>3</sup>). The corresponding CO<sub>2</sub> viscosities are 0.067 and 0.073 mPa·s respectively. Therefore, the corrected interface position is located closer to the well than when we neglect variations in density. The Dentz and Tartakovsky (2009a) approach gives a higher value of the mean CO<sub>2</sub> density because fluid pressure grows exponentially, while it grows linearly in Nordbotten et al. (2005) approach, thus leading to lower fluid pressure values in the zone where CO<sub>2</sub> and brine coexist. We define relative error,  $E_{rel}$ , of the interface position as

$$E_{rel} = \frac{R_i - R_c}{R_i}, \quad (21)$$

where  $R_i$  is the radius of the CO<sub>2</sub> plume at the top of the aquifer for incompressible CO<sub>2</sub> and  $R_c$  is the radius of the CO<sub>2</sub> plume at the top of the aquifer for compressible CO<sub>2</sub>.

Differences between the compressible and incompressible solutions are shown in Fig. 4. For the [Dentz and Tartakovsky \(2009a\)](#) solution, the relative error increases slightly from the base to the top of the aquifer, presenting a maximum relative error of 6% at the top of the aquifer. For the [Nordbotten et al. \(2005\)](#) solution the interface tilts, with the base of the interface located just 2% further from the well than its initial position, but the top positioned 7% closer to the well. The difference in shape between the two analytical solutions results in a CO<sub>2</sub> plume that extends further along the top of the aquifer for [Nordbotten et al. \(2005\)](#) solution than [Dentz and Tartakovsky \(2009a\)](#) over time (Fig. 4b). A similar behavior can be seen in the numerical simulations (Fig. 4a). In this case, the interface given by the numerical simulation compares favourably with that of [Nordbotten et al. \(2005\)](#).

Figure 4c displays a comparison between the vertically averaged fluid pressure given by both approaches. The fluid pressure given by [Mathias et al. \(2008\)](#) is almost identical to that obtained in [Nordbotten et al. \(2005\)](#) approach (Eq. (17)). This is because [Mathias et al. \(2008\)](#) assumed the [Nordbotten et al. \(2005\)](#) solution for the interface position and that the hypothesis made therein are valid. The minor difference in fluid pressure between these two expressions comes from considering a slight fluid and rock compressibility beyond the plume (recall Section 2). Thus, both expressions can be considered equivalent for the vertically averaged fluid pressure. Fluid pressure obtained from the numerical simulation is smaller than the other profiles inside the CO<sub>2</sub> plume region. This may reflect the larger energy dissipation produced by analytical solutions as a result of the Dupuit assumption.

### 5.3 Case 2: Comparable Gravity and Viscous Forces

Here, the gravity number at the well is in the order of  $10^{-1}$  (Note that the gravity number increases to 1 if we take a characteristic length only 1.5 m away from the injection well. In fact, it keeps increasing further away from the well, where gravity forces will eventually dominate (recall Section 2)). The density variations between the initial guess of 730 kg/m<sup>3</sup> and the corrected value can be large. The density reduces to 512 kg/m<sup>3</sup> (viscosity of 0.037 mPa-s) for [Nordbotten et al. \(2005\)](#) and to 493 kg/m<sup>3</sup> (viscosity of 0.036 mPa-s) for [Dentz and Tartakovsky \(2009a\)](#). This means that the error associated with neglecting CO<sub>2</sub> compressibility can become very large and should be reflected in the interface position (Fig. 5a). For the [Dentz and Tartakovsky \(2009a\)](#) solution including compressibility leads to a 26% error at the top of the aquifer. This relative error reaches 53% in the [Nordbotten et al. \(2005\)](#) solution. Over a 30 year injection this could represent a potential error of 3 km in the interface position estimation (Fig. 5b). Here, the numerical simulations also show the importance of considering CO<sub>2</sub> compressibility. The interface position from the simulations is similar to that of [Nordbotten et al. \(2005\)](#) in the lower half of the aquifer, where viscous forces may dominate, but it is similar to that of [Dentz and Tartakovsky \(2009a\)](#) in the upper part of the aquifer, where buoyancy begins to dominate.

This dominant buoyancy flow may be significant when considering risks associated with potential leakage from the aquifer ([Nordbotten et al. 2009](#)) or mechanical damage of the caprock ([Vilarrasa et al. 2010](#)), where the extent and pressure distribution of the CO<sub>2</sub> on the top of the aquifer plays a dominant role.

Unlike the previous case, the mean CO<sub>2</sub> density of [Dentz and Tartakovsky \(2009a\)](#) approach is lower than that of [Nordbotten et al. \(2005\)](#). This is because [Nordbotten et al. \(2005\)](#) consider the vertically averaged fluid pressure (Fig. 5c). When gravity forces play an

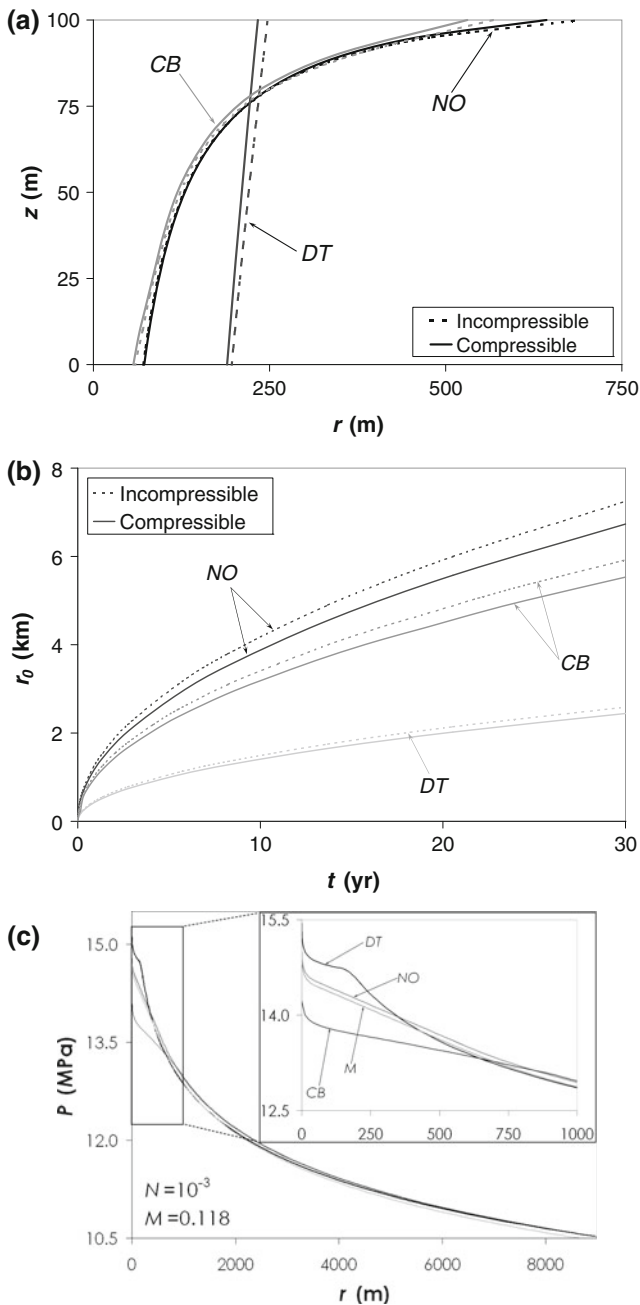


**Fig. 4** Case 1: Viscous forces dominate. Gravity number,  $N$ , equals  $10^{-3}$  in the well. (a) Abrupt interface position in a vertical cross section after 100 days of injection, (b) evolution of the CO<sub>2</sub> plume radius at the top of the aquifer and (c) vertically averaged fluid pressure with distance to the well after 100 days of injection, with a detail of the CO<sub>2</sub> rich zone. *NO* refers to Nordbotten et al. (2005) solution, *DT* to Dentz and Tartakovsky (2009a) solution, *CB* to the numerical solution of CODE\_BRIGHT and *M* is the Mathias et al. (2008) solution for fluid pressure

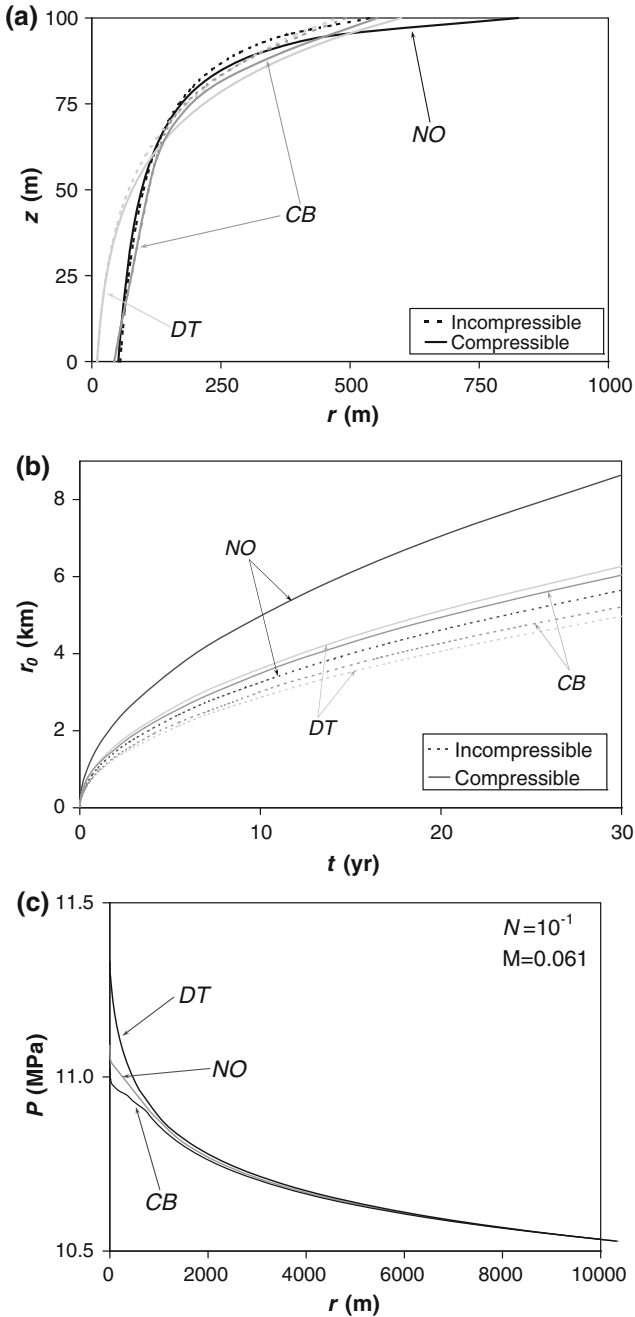


**Fig. 5** Case 2: Comparable viscous and gravity forces. Gravity number,  $N$ , equals  $10^{-1}$  in the well. (a) Abrupt interface position in a vertical cross section after 100 days of injection, (b) evolution of the CO<sub>2</sub> plume radius at the top of the aquifer and (c) vertically averaged fluid pressure with distance to the well after 100 days of injection. *NO* refers to Nordbotten et al. (2005) solution, *DT* to Dentz and Tartakovsky (2009a) solution and *CB* to the numerical solution of CODE\_BRIGHT

important role, the CO<sub>2</sub> plume largely extends at the top of the aquifer. CO<sub>2</sub> pressure at the top of the aquifer is lower than the vertically averaged fluid pressure, which considers CO<sub>2</sub> and the formation brine. Thus, the mean CO<sub>2</sub> density is overestimated when it is calculated from vertically averaged fluid pressure values.

#### 5.4 Case 3: Gravity Forces Dominate

In this case, the gravity number is close to 10 at the well. Density deviations from our initial guess can be very large here. The mean density drops to 479 kg/m<sup>3</sup> for Nordbotten et al. (2005) and to 449 kg/m<sup>3</sup> for Dentz and Tartakovsky (2009a) solutions, which correspond to CO<sub>2</sub> viscosities of 0.035 and 0.032 mPa·s respectively. This means that the interface position at the top of the aquifer will extend much further than when not considering CO<sub>2</sub> compressibility. The Dentz and Tartakovsky (2009a) solution clearly reflects buoyancy and the CO<sub>2</sub> advances through a very thin layer at the top of the aquifer (Fig. 6a). In contrast, the Nordbotten et al. (2005) interface cannot represent this strong buoyancy effect because this solution does not account for gravitational forces. The relative error of the interface position at the top of the aquifer is of 30% for Dentz and Tartakovsky (2009a) solution, and of 64% for Nordbotten et al. (2005). In this case, the numerical simulation compares more favourably with the Dentz and Tartakovsky (2009a) solution.

The vertically averaged pressure from Dentz and Tartakovsky (2009a) is similar to that of the numerical simulation because gravity forces dominate (Fig. 6c). In this case, Nordbotten et al. (2005) predict a very small pressure buildup, which reflects their linear variation with distance. In addition, the zone with only CO<sub>2</sub>, where fluid pressure grows logarithmically, is very limited.

Finally, we consider the influence of the gravity number on CO<sub>2</sub> compressibility effects. Figure 7 displays the relative error (Eq. 21) of the interface position at the top of the aquifer as a function of the gravity number, computed at the injection well. Negative relative errors mean that the interface position extends further when considering CO<sub>2</sub> compressibility. Both analytical solutions, i.e. Nordbotten et al. (2005) and Dentz and Tartakovsky (2009a), present a similar behaviour, but Nordbotten et al. (2005) has a bigger error. This is mainly because they vertically average fluid pressure, which leads to unrealistic CO<sub>2</sub> properties in the zone where both CO<sub>2</sub> and brine exist. For gravity numbers greater than 1, the mean CO<sub>2</sub> density tends to a constant value because fluid pressure buildup in the well is very small. For this reason, the relative error remains constant for this range of gravity numbers. However, the absolute relative error decreases until the mean CO<sub>2</sub> density equals that of the initial approximation for gravity numbers lower than 1. The closer the initial CO<sub>2</sub> density approximation is to the actual density, the smaller is the error in the interface position.

Figure 8 displays the mean CO<sub>2</sub> density as a function of the gravity number computed in the well for the cases discussed here. Differences arise between the two analytical approaches. The most relevant difference occurs at high gravity numbers. For gravity numbers greater than  $5 \times 10^{-2}$ , Nordbotten et al. (2005) yield a higher CO<sub>2</sub> density because fluid pressure is averaged over the whole vertical. Thus, fluid pressure in the zone where CO<sub>2</sub> and brine exist is overestimated, resulting in higher CO<sub>2</sub> density values. For gravity numbers lower than  $5 \times 10^{-2}$ , CO<sub>2</sub> density given by Dentz and Tartakovsky (2009a) is slightly higher than that of Nordbotten et al. (2005) because the former predicts higher fluid pressure values in the CO<sub>2</sub>-rich zone, as explained previously. However, both approaches present similar mean CO<sub>2</sub> density values for low gravity numbers.



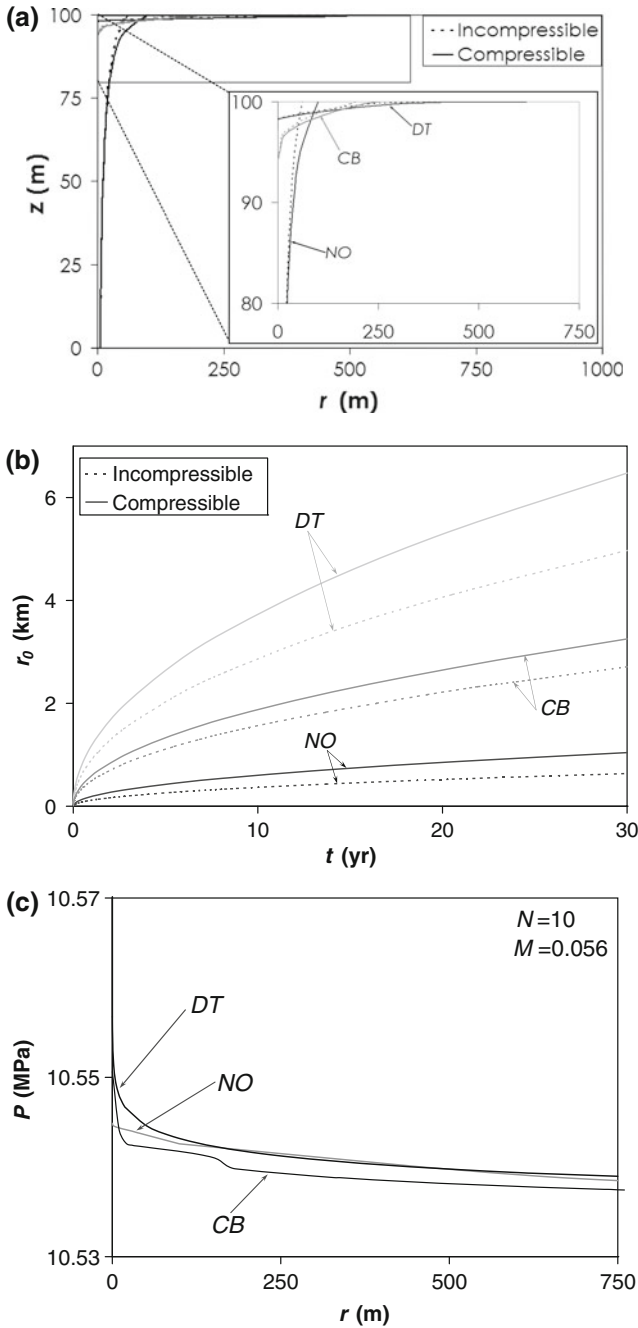


**Fig. 6** Case 3: Gravity forces dominate. Gravity number,  $N$ , equals 10 in the well. (a) Abrupt interface position in a vertical cross section after 100 days of injection, (b) evolution of the CO<sub>2</sub> plume radius at the top of the aquifer and (c) vertically averaged fluid pressure with distance to the well after 100 days of injection. *NO* refers to Nordbotten et al. (2005) solution, *DT* to Dentz and Tartakovsky (2009a) solution and *CB* to the numerical solution of CODE\_BRIGHT

**Fig. 7** Relative error (Eq. 21) of the interface position at the top of the aquifer made when  $\text{CO}_2$  compressibility is not considered as a function of the gravity number for both analytical solutions. *NO* refers to Nordbotten et al. (2005) solution and *DT* to Dentz and Tartakovsky (2009a) solution

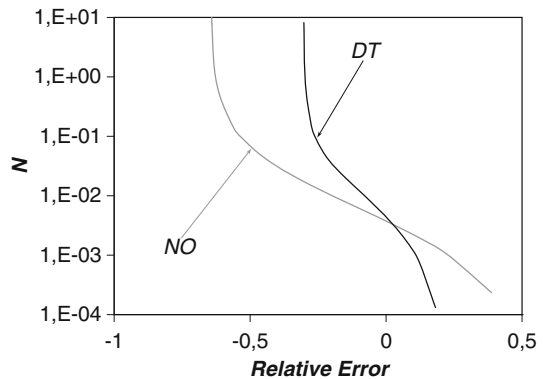
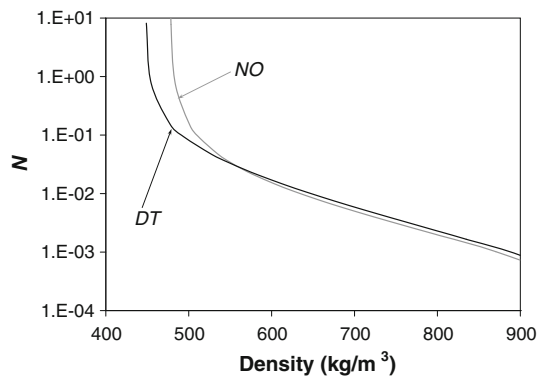


**Fig. 8** Mean  $\text{CO}_2$  density as a function of the gravity number in the cases discussed here for both analytical solutions. *NO* refers to Nordbotten et al. (2005) solution and *DT* to Dentz and Tartakovsky (2009a) solution



## 6 Summary and Conclusions

$\text{CO}_2$  compressibility effects may play an important role in determining the size and geometry of the  $\text{CO}_2$  plume that will develop when supercritical  $\text{CO}_2$  is injected in an aquifer. Here, we have studied the effect that accounting for  $\text{CO}_2$  compressibility (density variations and corresponding changes in viscosity) exerts on the shape of the plume computed by two abrupt interface analytical solutions. To this end, we have presented a simple method to correct the initial estimation of the  $\text{CO}_2$  density and viscosity, and hence use more realistic values. These corrected values give a more accurate prediction for the interface position of the  $\text{CO}_2$  plume.

The error associated with neglecting compressibility increases dramatically when gravity forces dominate, which is likely to occur at late injection times. This is relevant because the relative importance of buoyancy forces increases with distance to the injection well. Thus gravity forces will ultimately dominate in most  $\text{CO}_2$  sequestration projects. As such incorporating  $\text{CO}_2$  compressibility is critical for determining the interface position.

Comparison with numerical simulations suggests that the solution by Nordbotten et al. (2005) gives good predictions when viscous forces dominate, while the Dentz and Tartakovsky (2009a) solution provides good estimates of the  $\text{CO}_2$  plume position when gravity forces dominate.

**Acknowledgements** V.V. and D.B. want to acknowledge the Spanish Ministry of Science and Innovation (MCI) for financial support through the “Formación de Profesorado Universitario” and “Juan de la Cierva” programs. V.V. also wants to acknowledge the “Colegio de Ingenieros de Caminos, Canales y Puertos-

Catalunya” for their financial support. Additionally, we would like to acknowledge the ‘CIUDEN’ project (Ref.: 030102080014), the ‘PSE’ project (Ref.: PSE-120000-2008-6), the ‘COLINER’ project and the ‘MUS-TANG’ project (from the European Community’s Seventh Framework Programme FP7/2007-2013 under grant agreement no. 227286) for their financial support.

## 7 Appendix A

Here, the mean CO<sub>2</sub> density defined in (16) is calculated using the linear approximation of CO<sub>2</sub> density with respect to pressure presented in (20) for both approaches, i.e. Nordbotten et al. (2005) and Dentz and Tartakovsky (2009a).

With the Nordbotten et al. (2005) approach, the mean CO<sub>2</sub> density is calculated by introducing (11) and (17) into (16), which leads to

$$\bar{\rho}_{\text{CN}} = \frac{2\pi\phi}{V} \left\{ \rho_0 \frac{d}{2} r_0 r_b + \rho_1 \beta \left[ \frac{r_0 r_b}{4} \rho_w g d^2 + \frac{Q_0 \mu_w}{2\pi k} \left[ r_0 r_b \left( \frac{1}{2} \ln \left( \frac{R}{r_0} \right) + \frac{1}{3} \right) - \frac{r_b^2}{6} \left( 1 - \frac{1}{2} \frac{\mu_c}{\mu_w} \right) \right] \right] \right\}. \quad (22)$$

Similarly, introducing (13) and (18) into (16), and integrating, yields the expression for the mean CO<sub>2</sub> density for the Dentz and Tartakovsky (2009a) approach,

$$\bar{\rho}_{\text{CDT}} = \frac{2\pi\phi}{V} \left\{ \left( e^{(2/\gamma_{\text{cw}})} - 1 \right) \frac{r_b^2}{4} d \gamma_{\text{cw}} \left[ \rho_0 + \rho_1 \beta \left( \frac{d \gamma_{\text{cw}}}{2} \rho_w g + \frac{Q_0}{2\pi k d} \left( \mu_w \ln \left( \frac{R}{r_b} \right) + \frac{\mu_w + \mu_c}{2} \right) \right) \right] - \frac{r_b^2}{4} d^2 \gamma_{\text{cw}} \rho_1 \beta \rho_w g - e^{(2/\gamma_{\text{cw}})} \frac{r_b^2}{4} d \rho_1 \beta \frac{Q_0}{2\pi k d} \mu_w \right\}. \quad (23)$$

## References

- Altunin, V.V., Sakhabetdinov, M.A. Viscosity of liquid and gaseous carbon dioxide at temperatures 220–1300 K and pressure up to 1200 bar. *Teploenergetika*, **8**, 85–89 (1972)
- Angus, A., Armstrong, B., Reuck, K.M. (eds.): International thermodynamics tables of the fluid state. Carbon dioxide. International Union of Pure and Applied Chemistry. Pergamon Press, Oxford (1976)
- Aziz, K., Settari, A. (eds.): Petroleum Reservoir Simulation. 2nd edn. Blitzzprint Ltd., Calgary (2002)
- Bachu, S.: Screening and ranking of sedimentary basins for sequestration of CO<sub>2</sub> in geological media in response to climate change. *Environ. Geol.* **44**, 277–289 (2003)
- Bachu, S., Adams, J.J.: Sequestration of CO<sub>2</sub> in geological media in response to climate change: capacity of deep saline aquifers to sequester CO<sub>2</sub> in solution. *Energy Convers. Manag.* **44**, 3151–3175 (2003)
- Bear, J. (ed.): Dynamics of Fluids in Porous Media. Elsevier, New York (1972)
- Bolster, D., Barahona, M., Dentz, M., Fernandez Garcia, D., Sanchez-Vila, X., Trichero, P., Volhondo, C., Tartakovsky, D.M.: Probabilistic risk assessment applied to contamination scenarios in porous media. *Water Resour. Res.* **45**, w06413. (2009a) doi:10.1029/2008wR007551
- Bolster, D., Dentz, M., Carrera, J.: Effective two phase flow in heterogeneous media under temporal pressure fluctuations. *Water Resour. Res.* **45**, W05408 (2009b). doi:10.1029/2008WR007460
- Cantucci, B., Montegrossi, G., Vaselli, O., Tassi, F., Quattrocchi, F., Perkins, E.H.: Geochemical modeling of CO<sub>2</sub> storage in deep reservoirs: the Weyburn Project (Canada) case study. *Chem. Geol.* **265**, 181–197 (2009)
- Celia, M.A., Nordbotten, J.M.: Practical modeling approaches for geological storage of carbon dioxide. *Ground Water* **47**(5), 627–638 (2009)

- Chen, Z., Huan, G., Ma, Y. (eds.): Computational methods for multiphase flows in porous media. SIAM, Philadelphia (2006)
- Cooper, H.H., Jacob, C.E.: A generalized graphical method for evaluating formation constants and summarizing well field history. *Am. Geophys. Union Trans.* **27**, 526–534 (1946)
- Dake, L.P. (ed.): *Fundamentals of Reservoir Engineering*. Elsevier, Oxford (1978)
- Dentz, M., Tartakovsky, D.M.: Abrupt-interface solution for carbon dioxide injection into porous media. *Trans. Porous Media* **79**, 15–27 (2009a)
- Dentz, M., Tartakovsky, D.M.: Response to “Comments on abrupt-interface solution for carbon dioxide injection into porous media by Dentz and Tartakovsky (2008)” by Lu et al. *Trans. Porous Media* **79**, 39–41 (2009b)
- Ennis-King, J., Paterson, L.: The role of convective mixing in the long-term storage of carbon dioxide in deep saline formations. *J. Soc. Pet. Eng.* **10**(3), 349–356 (2005)
- Garcia, J.E.: Fluid Dynamics of Carbon Dioxide Disposal into Saline Aquifers. PhD thesis, University of California, Berkeley (2003)
- Garcia, J.E., Pruess, K.: Flow Instabilities during injection of CO<sub>2</sub> into saline aquifers. Proceedings Tough Symposium 2003, LBNL, Berkeley (2003)
- GHS: Spreadsheet with CO<sub>2</sub> compressibility correction. <http://www.h2geo.upc.es/publicaciones/2009/Transport%20in%20porous%20media/Effects%20of%20CO2%20Compressibility%20on%20CO2%20Storage%20in%20Deep%20Saline%20Aquifers.xls> (2009)
- Hesse, M.A., Tchelepi, H.A., Cantwell, B.J., Orr, F.M. Jr.: Gravity currents in horizontal porous layers: Transition from early to late self-similarity. *J. Fluid Mech.* **577**, 363–383 (2007)
- Hesse, M.A., Tchelepi, H.A., Orr, F.M. Jr.: Gravity currents with residual trapping. *J. Fluid Mech.* **611**, 35–60 (2008)
- Hidalgo, J.J., Carrera, J.: Effect of dispersion on the onset of convection during CO<sub>2</sub> sequestration. *J. Fluid Mech.* **640**, 443–454 (2009)
- Hitchon, B., Gunter, W.D., Gentzis, T., Bailey, R.T.: Sedimentary basins and greenhouse gases: a serendipitous association. *Energy Convers. Manag.* **40**, 825–843 (1999)
- Huppert, H.E., Woods, A.W.: Gravity-driven flows in porous media. *J. Fluid Mech.* **292**, 55–69 (1995)
- Juanes, R., MacMinn, C.W., Szulczewski, M.L.: The footprint of the CO<sub>2</sub> plume during carbon dioxide storage in saline aquifers: storage efficiency for capillary trapping at the basin scale. *Trans. Porous Media*. doi:[10.1007/s11242-009-9420-3](https://doi.org/10.1007/s11242-009-9420-3) (2009)
- Katz, D.L., Lee, R.L. (eds.): *Natural Gas Engineering*. McGraw-Hill, New York (1990)
- Kopp, A., Class, H., Helmig, R.: Investigation on CO<sub>2</sub> storage capacity in saline aquifers Part 1. Dimensional analysis of flow processes and reservoir characteristics. *J. Greenh. Gas Control* **3**, 263–276 (2009)
- Korbol, R., Kaddour, A.: Sleipner vest CO<sub>2</sub> disposal— injection of removed CO<sub>2</sub> into the Utsira formation. *Energy Convers. Manag.* **36**(6–9), 509–512 (1995)
- Lake, L.W. (ed.): *Enhanced Oil Recovery*. Prentice-Hall, Englewood Cliffs, New Jersey (1989)
- Law, D.H.S., Bachu, S.: Hydrogeological and numerical analysis of CO<sub>2</sub> disposal in deep aquifers in the Alberta sedimentary basin. *Energy Convers. Manag.* **37**(6–8), 1167–1174 (1996)
- Lu, C., Lee, S.-Y., Han, W.S., McPherson, B.J., Lichtner, P.C.: Comments on “abrupt-interface solution for carbon dioxide injection into porous media” by M. Dentz and D. Tartakovsky. *Trans. Porous Media* **79**, 29–37 (2009)
- Lyle, S., Huppert, H.E., Hallworth, M., Bickle, M., Chadwick, A.: Axisymmetric gravity currents in a porous medium. *J. Fluid Mech.* **543**, 293–302 (2005)
- Mathias, S.A., Hardisty, P.E., Trudell, M.R., Zimmerman, R.W.: Approximate solutions for pressure buildup during CO<sub>2</sub> injection in brine aquifers. *Trans. Porous Media*. doi:[10.1007/s11242-008-9316-7](https://doi.org/10.1007/s11242-008-9316-7) (2008)
- McPherson, B.J.O.L., Han, W.S., Cole, B.S.: Two equations of state assembled for basic analysis of multiphase CO<sub>2</sub> flow and in deep sedimentary basin conditions. *Comput. Geosci.* **34**, 427–444 (2008)
- Neuweiller, I., Attinger, S., Kinzelbach, W., King, P.: Large scale mixing for immiscible displacement in heterogeneous porous media. *Trans. Porous Media* **51**, 287–314 (2003)
- Neuzil, C.E.: Groundwater flow in low-permeability environments. *Water Resour. Res.* **22**(8), 1163–1195 (1986)
- Nooner, S.L., Eiken, O., Hermanrud, C., Sasagawa, G.S., Stenvold, T., Zumberge, M.A.: Constraints on the in situ density of CO<sub>2</sub> within the Utsira formation from time-lapse seafloor gravity measurements. *J. Greenh. Gas Control* **1**, 198–214 (2007)
- Nordbotten, J.M., Celia, M.A., Bachu, S.: Injection and storage of CO<sub>2</sub> in deep saline aquifers: analytical solution for CO<sub>2</sub> plume evolution during injection. *Trans. Porous Media* **58**, 339–360 (2005)
- Nordbotten, J.M., Kavetski, D., Celia, M.A., Bachu, S.: A semi-analytical model estimating leakage associated with CO<sub>2</sub> storage in large-scale multi-layered geological systems with multiple leaky wells. *Environ. Sci. Technol.* **43**(3), 743–749 (2009). doi:[10.1021/es801135v](https://doi.org/10.1021/es801135v)

- Olivella, S., Carrera, J., Gens, A., Alonso, E.E.: Non-isothermal multiphase flow of brine and gas through saline media. *Trans. Porous Media* **15**, 271–293 (1994)
- Olivella, S., Gens, A., Carrera, J., Alonso, E.E.: Numerical formulation for a simulator (CODE\_BRIGHT) for the coupled analysis of saline media. *Eng. Comput.* **13**, 87–112 (1996)
- Pruess, K., Garcia, J.: Multiphase flow dynamics during CO<sub>2</sub> disposal into saline aquifers. *Environ. Geol.* **42**, 282–295 (2002)
- Pruess, K., Garcia, J., Kovscek, T., Oldenburg, C., Rutqvist, J., Steelfel, C., Xu, T.: Code intercomparison builds confidence in numerical simulation models for geologic disposal of CO<sub>2</sub>. *Energy* **29**, 1431–1444 (2004)
- Riaz, A., Hesse, M., Tchelepi, H., Orr, F.M. Jr.: Onset of convection in a gravitationally unstable diffusive boundary layer in porous media. *J. Fluid Mech.* **548**, 87–111 (2006)
- Rutqvist, J., Birkholzer, J., Cappa, F., Tsang, C.-F.: Estimating maximum sustainable geological sequestration of CO<sub>2</sub> using coupled fluid flow and geomechanical fault-slip analysis. *Energy Convers. Manag.* **48**, 1798–1807 (2007)
- Saripalli, P., McGrail, P.: Semi-analytical approaches to modeling deep well injection of CO<sub>2</sub> for geological sequestration. *Energy Convers. Manag.* **43**, 185–198 (2002)
- Sovova, H., Prochazka, J.: Calculations of compressed carbon dioxide viscosities. *Ind. Eng. Chem. Res.* **32**(12), 3162–3169 (1993)
- Span, R., Wagner, W.: A new equation of state for carbon dioxide covering the fluid region from the triple-point to 1100 K at pressures up to 88 MPa. *J. Phys. Chem. Ref. Data* **25**(6), 1509–1596 (1996)
- Stauffer, P.H., Viswanathan, H.S., Pawar, R.J., Guthrie, G.D.: A system model for geologic sequestration of carbon dioxide. *Environ. Sci. Technol.* **43**(3), 565–570 (2009)
- Tartakovsky, D.M.: Probabilistic risk analysis in subsurface hydrology. *Geophys. Res. Lett.* **34**, L05 404 (2007)
- Tchelepi, H.A., Orr, F.M. Jr.: Interaction of viscous fingering, permeability inhomogeneity and gravity segregation in three dimensions. *SPE Symposium on Reservoir Simulation*, New Orleans, pp. 266–271, (1994)
- Thiem, G. (ed.): *Hydrologische Methode*. Leipzig, Gebhardt (1906)
- Tsang, C.-F., Birkholzer, J., Rutqvist, J.: A comparative review of hydrologic issues involved in geologic storage of CO<sub>2</sub> and injection disposal of liquid waste. *Environ. Geol.* **54**, 1723–1737 (2008)
- van Genuchten, M.T.: A closed-form equation for predicting the hydraulic conductivity of unsaturated soils. *Soil. Sci. Soc. Am. J.* **44**, 892–898 (1980)
- Vilarrasa, V., Bolster, D., Olivella, S., Carrera, J.: Coupled hydromechanical modelling of CO<sub>2</sub> sequestration in deep saline aquifers. *Int. J. Greenh. Gas Control* (submitted) (2010)
- Zhou, Q., Birkholzer, J., Tsang, C.-F., Rutqvist, J.: A method for quick assessment of CO<sub>2</sub> storage capacity in closed and semi-closed saline formations. *J. Greenh. Gas Control* **2**, 626–639 (2008)